Heliyon 5 (2019) e02370

Contents lists available at ScienceDirect

Heliyon

journal homepage: www.heliyon.com

Sustained antigen release polyanhydride-based vaccine platform for immunization against bovine brucellosis

Paola M. Boggiatto [a,*], Robert G. Schaut [b], Carly Kanipe [a], Sean M. Kelly [c], Balaji Narasimhan [c,e], Douglas E. Jones [d,e], Steven C. Olsen [a]

[a] Infectious Bacterial Diseases Research Unit, National Animal Disease Centers, United States Department of Agriculture, 1920 Dayton Avenue, Ames, IA, 50010, USA
[b] Food Safety and Enteric Pathogens Research Unit, National Animal Disease Centers, United States Department of Agriculture, 1920 Dayton Avenue, Ames, IA, 50010, USA
[c] Department of Chemical and Biological Engineering, Iowa State University, 618 Bissell Road, Ames, IA, 50010, USA
[d] Department of Veterinary Pathology, Iowa State University, 1800 Christensen Drive, Ames, IA, 50010, USA
[e] Nanovaccine Institute, Iowa State University, Ames, IA, 50010, USA

ARTICLE INFO

Keywords:
Immunology
Infectious disease
Vaccines
Immune response
Vaccination
Antibody
Bacteria
Polyanhydride
Vaccine
Cattle
Single-dose
Brucella

ABSTRACT

Brucellosis is a bacterial zoonosis and a significant source of economic loss and a major public health concern, worldwide. Bovine brucellosis, as caused primarily by *Brucella abortus*, is an important cause of reproductive loss in cattle. Vaccination has been the most effective way to reduce disease prevalence contributing to the success of control and eradication programs. Currently, there are no human vaccines available, and despite the success of commercial vaccines for livestock, such as *B. abortus* strain RB51 (RB51), there is need for development of novel and safer vaccines against brucellosis. In the current study, we report the fabrication of and immune responses to an implantable single dose polyanhydride-based, methanol-killed RB51 antigen containing delivery platform (VPEAR) in cattle. In contrast to animals vaccinated with RB51, we did not observe measurable RB51-specific IFN-γ or IgG responses in the peripheral blood, following initial vaccination with VPEAR. However, following a subsequent booster vaccination with RB51, we observed an anamnestic response in both vaccination treatments (VPEAR and live RB51). The magnitude and kinetics of CD4+ IFN-γ-mediated responses and circulating memory T cell subpopulations were comparable between the two vaccination treatments. Additionally, IgG titers were significantly increased in animals vaccinated with VPEAR as compared to live RB51- vaccinated animals. These data demonstrate that killed antigen may be utilized to generate and sustain memory, IFN-γ-mediated, CD4+ T cell and humoral responses against Brucella in a natural host. To our knowledge, this novel approach to vaccination against intracellular bacteria, such as *Brucella*, has not been reported before.

1. Introduction

Brucellosis is a zoonosis caused by bacteria of the genus *Brucella*. Worldwide, brucellosis is a significant source of economic losses and a major public health concern. In humans, brucellosis can result in a chronic debilitating disease while in domestic species (cattle, goats, sheep) brucellosis results in infertility and reproductive losses. In cattle, brucellosis is primarily caused by *Brucella abortus* and vaccination is a major factor in the success of control and eradication programs (reviewed in (Olsen and Stoffregen, 2005)). Commercially-available cattle vaccines against *B. abortus* include RB51 and S19, however, safe and effective vaccines for humans (and other domestic species) are currently not available. The RB51 vaccine is a lipopolysaccharide O-antigen-deficient rough mutant derived from *B. abortus* 2308, a smooth, virulent field strain. RB51 has been demonstrated to provide long-lasting immunity and protection against infection with field strains of *B. abortus* in cattle (Cheville et al., 1996; Cheville et al., 1993; Olsen, 2000; Poester et al., 2006). In addition, RB51 does not induce serologic responses that interfere with brucellosis surveillance tests (Schurig et al., 1991). However, RB51 has some drawbacks. Although less virulent than other vaccine strains and generally safe for use in pregnant cattle (Palmer et al., 1997), RB51 can be abortigenic (Yazdi et al., 2009). Additionally, recent reports have shown that RB51 can be shed in milk of previously-vaccinated cattle and infect humans through the consumption

* Corresponding author.
E-mail address: paola.boggiatto@ars.usda.gov (P.M. Boggiatto).

https://doi.org/10.1016/j.heliyon.2019.e02370
Received 26 February 2019; Received in revised form 26 July 2019; Accepted 22 August 2019

of unpasteurized milk (Cossaboom et al., 2018). This zoonotic potential raises important public health concerns as the RB51 strain is resistant to rifampicin, the antibiotic of choice for treating human brucellosis (Marianelli et al., 2004). Due to these drawbacks and the lack of safe and efficacious vaccines for other species, there is continued interest for development of novel vaccines that may be used to prevent brucellosis in animals and humans.

Brucella spp. are facultative intracellular pathogens, which reside within macrophages and can set up long-term residence within infected cells. Immunity against intracellular pathogens is considered to be primarily mediated by T helper (T_H)-1 responses, characterized by interferon-gamma (IFN-γ)-producing $CD4^+$ and $CD8^+$ T cells. Live *Brucella* vaccines have been shown to be far superior to inactivated vaccines for protection against infection (Montaraz and Winter, 1986; Zhan et al., 1993, 1995). Interestingly, while heat-killed preparations of *Brucella* can act as T_H1-promoting adjuvants (Huang et al., 1999, 2003, 2005), killed *Brucella* are unable to confer protection against challenge (Zhan et al., 1993, 1995). Moreover, both killed and live vaccines promote humoral responses, yet only live bacteria promote the development of memory IFN-γ-producing $CD4^+$ T cells (Vitry et al., 2014). These data suggest that the nature (i.e. live vs. killed antigen), as well as persistence and localization of antigen, may be key factors in promoting protective immunity against *Brucella* infection.

Concomitant immunity, or non-sterile immunity, is characterized by the ability of a host to mount an effective immune response against an organism without resulting in its complete clearance (Coffman et al., 2010; Perignon and Druilhe, 1994; Smith et al., 1999). *Leishmania major* and *Plasmodium falciparum* are both examples of organisms that promote concomitant immunity. During *L. major* infection, small numbers of parasites remain within the original site of infection and the draining lymph node (Nicolas et al., 2000). Resulting concomitant immunity is driven by a small pool of replicating parasites, from which some are destroyed and serve to provide a life-long supply of antigen stimulation to the host (Mandell and Beverley, 2017). Complete removal of these parasites by the host immune response results in loss of immunity (Belkaid et al., 2002). We hypothesize that a vaccination platform that mimics this long-term antigen release in the presence of inflammatory signals could generate protective and long-lived responses against persistent intracellular pathogens, such as *Brucella* spp. without inducing tolerance.

Polyanhydrides (PA) are biodegradable polymers that have been previously shown to be safe (Huntimer et al., 2013; Vela-Ramirez et al., 2015) and efficacious as delivery platforms for vaccine antigens (Carrillo-Conde et al., 2010; Petersen et al., 2009; Ross et al., 2015; Torres et al., 2006; Ulery et al., 2011a,b). Their effectiveness is centered around their ability to protect their payload (i.e. antigen) from degradation (Carrillo-Conde et al., 2010; Haughney et al., 2013; Ross et al., 2014; Vela Ramirez et al., 2014), their immune-enhancing nature (i.e. pathogen-mimicking) (Ulery et al., 2011b), and the ability to modulate antigen release by altering the degradation characteristics of the polymer chemistry (Carrillo-Conde et al., 2010; Petersen et al., 2009; Ross et al., 2015; Torres et al., 2006; Ulery et al., 2011a). Polyanhydride co-polymers consisting of 1,8-bis(*p*carboxyphenoxy)-3,6-dioxaoctane (CPTEG) and 1,6-bis(*p*-carboxyphenoxy)hexane (CPH), in a 20:80 ratio (i.e. 20:80 CPTEG:CPH), have been previously assessed for their ability to entrap proteins and for their low surface erosion properties, which allows for continuous antigen release (Torres et al., 2006; Vela-Ramirez et al., 2015).

In this study, we report the fabrication of an implantable single dose 20:80 CPTEG:CPH polymer-based, methanol-killed RB51 antigen-containing vaccine platform for extended antigen release (VPEAR). The rationale behind VPEAR is to provide the immune system with a three-hit model of antigen delivery to mimic the mechanism driving concomitant immunity: (1) a soluble component, which initially primes the immune system, (2) a boosting dose of antigen, provided by surface erosion and degradation of a solid polyanhydride rod over 3 months, and (3) a sustained release of antigen over a longer period of time (within 38 months) using a solid polyanhydride rod within a polyethylene implant, capped with a PVDF membrane (Schaut et al., 2018b). Inclusion of the PVDF membrane (0.65 μm pore size) restricts cells from accessing the antigen depot, yet allows antibody entry into the implant. The PVDF membrane caps a collagen immunodiffusion barrier overlaying the antigen depot, whereby the size of antigen-antibody complexes within the immunodiffusion barrier could theoretically provide a dynamic relationship between the immune response and antigen release.

In this study we assessed and compared the peripheral $CD4^+$ T cell and humoral immune responses to VPEAR and RB51 following initial vaccination and subsequent RB51 booster vaccination. Additionally, we characterize the histologic changes occurring at the site of VPEAR implantation.

2. Materials and methods

2.1. Polyanhydride formulations

20:80 CPTEG:CPH copolymer was synthesized using melt polycondensation as previously described (Torres et al., 2006). The molar composition and number-average molecular weight was determined via end group analysis of ^1H NMR spectra (DXR 500). Thermal properties of the polymer, including its glass transition temperature, were determined using differential scanning calorimetry (Q2000, TA Instruments). The 20:80 CPTEG:CPH copolymer had a molar composition of 21:79 (mol CPTEG:mol CPH), a number-average molecular weight of 6,111 g/mol, and a glass transition temperature of 29.7 °C, consistent with previous reports (Torres et al., 2006).

2.2. Methanol-killed RB51 antigen generation

Commercially-available RB51 vaccine (Colorado Serum Company, Denver, CO) was inoculated in *Brucella* broth (Becton Dickinson, Sparks, MD). The inoculum was incubated at 37 °C with constant shaking until reaching an optical density (OD) value of 1.5, equivalent to approximately 10^{10} colony forming units (CFU)/mL. After inactivation in 60% methanol for 7 days, loss of viability was confirmed by plating onto tryptose agar plates with 5% bovine serum and incubation for 7 days at 37 °C with 5% CO_2. After confirmation of inactivation, methanol-killed RB51 was centrifuged at 30,000 x g for 30 min at 4 °C to remove soluble media components. The pellet was resuspended in sterile, culture-grade Dulbecco's phosphate-buffered saline (DPBS), centrifuged again, resuspended in high-grade methanol, and stored at 4 °C until use.

2.3. Rod and implant design (VPEAR)

Polyanhydride (PA) rod and implant synthesis were performed as previously described (Schaut et al., 2018b). The rod consisted of 208 mg of PA, 1×10^{10} CFU of methanol-killed RB51, and 50 μg of MPLA derived from *Salmonella minnesota* R595 (InvivoGen, San Diego, CA). The rod that was placed in the implant consisted of 138 mg of PA, 1×10^{10} CFU of sonicated, methanol-killed RB51, and 50 μg of MPLA (InvivoGen). Air-dried mixtures of all components were pressed in a custom-made mold at 0.5 tons-on-ram for 5 s, using an International Crystal Laboratories hydraulic press. The implant was designed and formulated as previously described (Schaut et al., 2018a).

2.4. Animal vaccinations

Holstein steers, 6–8 months old, were housed in field barns at the National Animal Disease Centers (NADC) in Ames, IA. All experiments were approved by the NADC Institutional Animal Care and Use Committee (IACUC). Upon arrival, all steers were dewormed and vaccinated with Triangle 5 vaccine (Boehringer Ingleheim, Fort Dodge, IA). After acclimation, animals were randomly assigned to one of three treatment

groups: naïve (n = 6), live RB51 (n = 6), or VPEAR (n = 8). Naïve animals received 2 mL of phosphate buffered saline (PBS) subcutaneously (SQ) in the cervical region, using a 1 ½ inch 20-gauge needle. Animals in the RB51 group were SQ vaccinated with 3×10^{10} colony-forming units (CFU) of a commercial RB51 vaccine (Lot number 2639, Colorado Serum Company) in the cervical region using a 1 ½ inch, 20-gauge needle. In the VPEAR group, the implant and rod were surgically administered SQ along with a soluble injection of 1×10^{10} CFU of methanol-killed RB51, using a 1 ½ inch 20-gauge needle. Blood was collected via venipucture at 4-week intervals to track humoral and cellular responses. Booster vaccinations were performed at 10 months post-initial vaccination, SQ, with 3×10^{10} CFU of a commercial RB51 vaccine (Colorado Serum Company) in the cervical region using a 1 ½ inch 20-gauge needle. Blood was collected via venipuncture at 2, 4, and 8 weeks post-boost to track cellular responses and at 4 week intervals to track humoral responses. At the end of the study, animals were humanely euthanized via intravenous injection of pentobarbital sodium solution.

2.5. Peripheral blood mononuclear cells (PBMC) isolation and in vitro stimulation

PBMC were isolated from peripheral blood via Ficoll gradient separation as previously described (Olsen et al., 2009). After assessing numbers of viable cells by trypan blue exclusion, PBMC were plated onto 96-round bottom plates at a density of 1×10^6 cells per well and incubated at 37 °C with 5% CO_2 in media only, with γ-irradiated RB51 (1×10^7 CFU/well), or with pokeweed mitogen (PWM, 4 μg/mL) (Sigma-Aldrich, St. Louis, MO).

2.6. Surface marker staining

PBCM were prepared *ex vivo* for surface cell marker staining by washing in PBS, followed by incubation with a fixable viability dye (Invitrogen Molecular Probes/ThermoFisher) for 20 min at 4 °C, followed by a PBS wash step, and resuspension in FACS buffer (PBS with 0.5% FBS). Cells were incubated at room temperature (RT) with primary antibodies for mouse anti-bovine CD3 (IgG1; Washington State University) and mouse anti-bovine CD45RO (IgG3; Bio-Rad, Hercules, CA), for 15 min, followed by BV421-labeled rat anti-mouse IgG1 (BD Biosciences, San Jose, CA) and BUV395-labeled rat anti-mouse IgG3 (BD Biosciences) for 15 min. After two wash steps in FACS buffer, cells were labeled with FITC-labeled mouse anti-bovine CD4 (Bio-Rad), PE-Cy7-labeled rat anti-human CCR7 (BD Bioscience), and PE-Cy5-labeled mouse anti-human CD62L (Biolegend, San Diego, CA). After two additional wash steps in FACS buffer, cells were resuspended in stabilizing fixative (BD Bioscience). Data was collected using a FACS Aria II flow cytometer (BD Biosciences) and analyzed using FlowJo® software (Tree Star, Inc., Ashland, OR).

2.7. Intracellular cytokine staining (ICS)

To measure intracellular cytokine production, PBMC were treated with a 1x solution of eBioscience™ Protein Transport Inhibitor (ThermoFisher Scientific) overnight for 16 h prior to harvesting at 7 days post-stimulation. Cells were washed twice with PBS, stained for viability and surface markers as described above, and then fixed and permeabilized using the BD Cytofix/Cytoperm™ kit (BD Biosciences), in accordance with manufacturer's recommendations. Cells were then incubated with PE-labeled mouse anti-bovine IFN-γ for 30 min at 4 °C. After staining, cells were washed and resuspended in stabilizing fixative (BD Bioscience). Data was collected using a FACS Aria II flow cytometer (BD Biosciences) and analyzed using FlowJo® software (Tree Star, Inc.).

2.8. RB51-specific IgG serum ELISA

Blood was collected into tiger top tubes and serum obtained by centrifugation. Serum was stored at -20 °C until analysis. Humoral IgG responses to RB51 antigens were measured via enzyme-linked immunosorbent assay (ELISA), as described previously (Olsen et al., 2009), with some modifications. Briefly, 96-flat bottom plates were coated with 1×10^8 CFU of methanol-killed RB51 diluted in coating buffer (carbonate-bicarbonate buffer, pH 9.6) and incubated overnight at 4 °C. Blocking of wells was performed using SuperBlock (ThermoFisher) in accordance with manufacturer's recommendations. After washing 3 times with wash buffer (PBS with 0.05% Tween 20), serum samples were added in triplicate to wells at dilutions of 1:800, 1:1600, and 1:3200 and incubated at RT for 2 h. For titration curves, serum samples were assessed in triplicates at dilutions of 1:1600, diluted 1:12,800, 1:25,600, and 1:51,200.

Plates were washed and then incubated with peroxidase-conjugated rabbit anti-bovine IgG (H+L) (Jackson Immunoresearch laboratories, West Grove, PA; 1:25,000), rabbit anti-bovine IgG1, or rabbit anti-bovine IgG2 (Bethyl Labs, Montgomery, TX; 1:50,000) for 1 h at RT. Following a wash, plates were developed using the TMB Microwell Peroxidase Substrate System (ThermoFisher) in accordance with manufacturer recommendations. After incubation, the reaction was stopped with 0.18 M solution of sulfuric acid and absorbance was measured at 450 nm using a plate reader.

2.9. IgG avidity ELISA

ELISAs to measure avidity were performed as described above with minor modifications. All samples were tested at 1:1,600 dilution, in triplicate. After a wash step, samples were incubated with 3 M urea, 6 M urea or wash buffer for 10 min at RT. Plates were then incubated with peroxidase-conjugated rabbit anti-bovine IgG (H+L) (1:25,000, Jackson Immunoresearch laboratories) for 1 h at RT, followed by a wash step. Plates were then developed and measured as described above. Avidity index was calculated by the ratio of absorbance values from the 3 M and 6 M urea treatments to absorbance values from samples incubated in wash buffer.

2.10. Cytokine quantification via AlphaLISA

Culture supernatants from PBMC were harvested 48 h post-stimulation and stored at -80 °C until analysis. AlphaLISA kits were utilized to measure IFN-γ, IL-4, IL-10, and IL-17A according to manufacturer's recommendations (PerkinElmer, Waltham, MA).

2.11. Histology

At necropsy, sections of skin and subcutaneous tissue around the implant site were obtained and fixed in neutral, buffered 10% formaldehyde, embedded in paraffin, sectioned at 5 μm, and stained with hematoxylin and eosin.

2.12. Statistics

Statistical analyses were performed using ordinary one-way ANOVA with Bonferoni's multiple comparisons test to determine statistical differences between treatment groups at each time point, for both cytokine and titer data sets. We considered each time point to be an independent experiment, as assays were run and data was collected at individual time points throughout the experimental timeline. For pair-wise comparisons, a Student's t-test was used to determine statistical significance between groups. Area under the curve (AUC) values were calculated for all experimental groups at each of the timepoints analyzed. Statistical analysis for AUC values were performed using one-way ANOVA with Bonferoni's multiple comparisons test. All statistical calculations and analyses were performed using GraphPad Prism7 software (GraphPad, San Diego, CA). A p-value of <0.05 was considered statistically-significant.

3. Results

3.1. VPEAR implant site reaction

Subcutaneous surgical implantation of the VPEAR in the cervical region elicited mild, temporary (<48hr) swelling in some animals. No other clinical effects were observed during the course of the study.

3.2. Peripheral RB51-specific CD4$^+$ T cell IFN-γ responses

It has been previously shown that in cattle, CD4$^+$ T cells are the main source of IFN-γ production following RB51 vaccination (Dorneles et al., 2015). Therefore, we assessed the peripheral CD4$^+$ T cell recall response to RB51 from PBMC isolated at different time points during the study. The gating strategy and representative dot plots for the data are shown in Fig. 1A. Following vaccination, we observed a significant increase ($p \leq 0.05$) in the mean percentage of IFN-γ-producing CD4$^+$ T cells in peripheral blood of RB51 vaccinates at 4, 8 and 16-weeks post-vaccination (Fig. 1B, gray bars) compared to naïve and VPEAR-implanted animals. At 12 weeks post-vaccination, mean frequency of IFN-γ-producing CD4$^+$ T cells trended higher but did not vary significantly ($p \geq 0.05$) in RB51 vaccinates as compared to VPEAR or naïve animals. Interestingly, we did not observe any differences ($p \geq 0.05$) in the mean frequencies of IFN-γ-producing CD4$^+$ T cells between VPEAR and naïve animals (Fig. 1B, black and white bars). We speculated that the lack of a measurable peripheral response in VPEAR-vaccinated animals could be attributed to localization of killed antigen at the site of vaccination and/or draining lymph node. Since we did not expect killed antigen to disseminate systemically, we hypothesized that any responses present would not be found peripherally, and furthermore, if a localized cellular response were present, then a systemic stimulus (i.e. *in vivo* recall response) may allow us to detect a memory response in circulation.

To test this hypothesis, we boosted all vaccinated animals with live RB51 and measured peripheral CD4$^+$ IFN-γ responses. Following booster, the mean frequency of antigen-specific IFN-γ-producing CD4$^+$ T cells in PBMC begins to increase ($p \geq 0.05$) by 2 weeks post-boost, but is significantly increased ($p \leq 0.05$) at 4 weeks after booster vaccination in both VPEAR and RB51 groups compared to the naïve animals (Fig. 1C). This response to RB51 boost was short-lived, as the mean percentage of IFN-γ-producing CD4$^+$ T cells was comparable ($p \geq 0.05$) to naïve responses by 8 weeks after booster vaccination. The observed kinetics are consistent with the profile of an anamnestic response to RB51, as they occur much faster and are shorter lived when compared to the kinetics of the primary response to RB51 vaccination (Fig. 1B). Altogether, these data suggest that VPEAR-vaccinated animals can generate a memory, IFN-γ-mediated CD4$^+$ T cell response comparable to RB51 vaccination.

3.3. Assessment of memory CD4$^+$ T cell subpopulations

To further characterize the memory CD4$^+$ T cell response, we

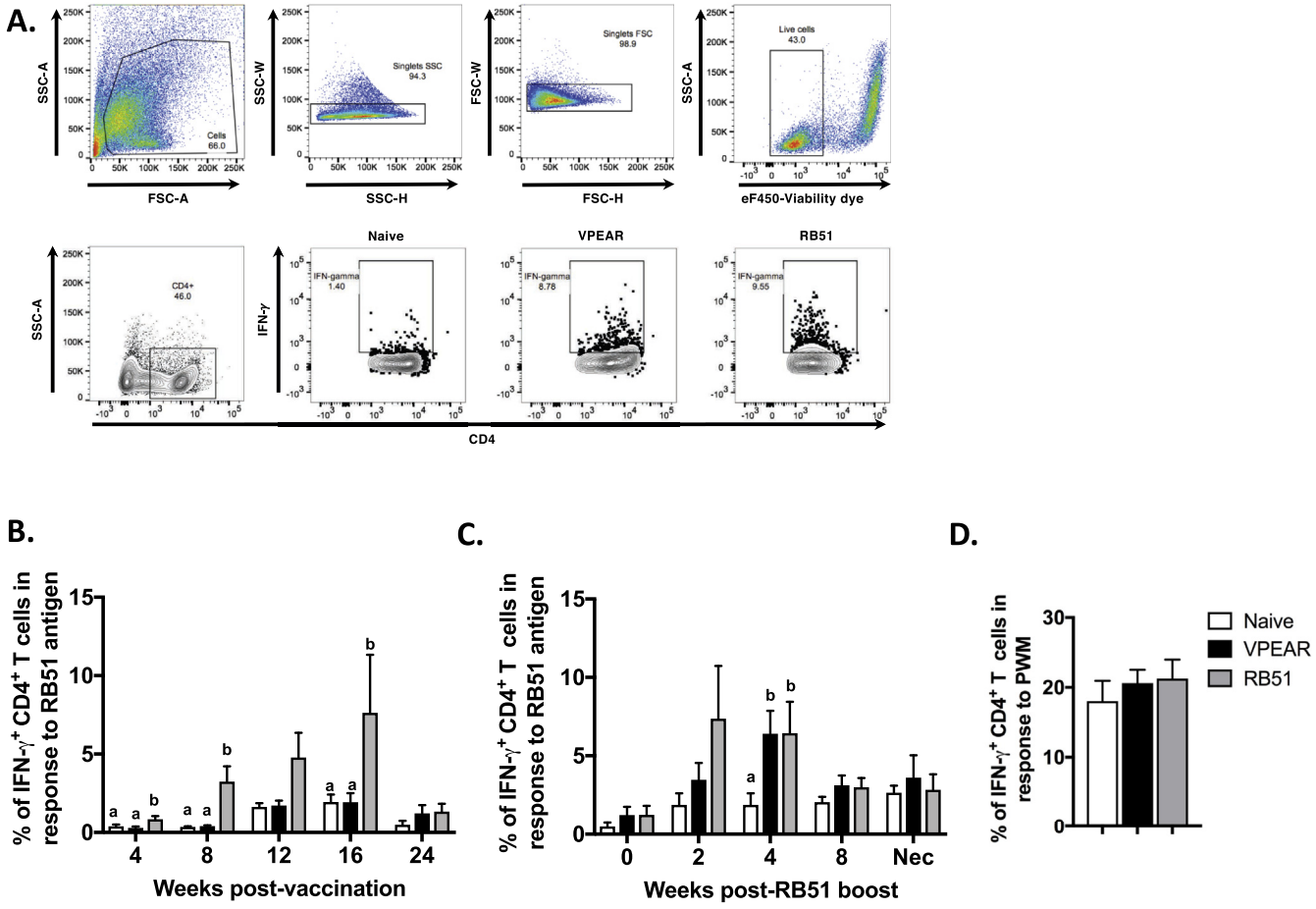

Fig. 1. Assessment of peripheral RB51-specific, IFN-γ production by CD4$^+$ T cells following VPEAR and RB51 vaccination and RB51 boost. (A) Representative dot plots showing FSC vs. SSC profile, gating strategy for singlet discrimination, viability assessment, and CD4 and intracellular IFN-γ staining on bovine PBMC. Time course showing the frequency of IFN-γ$^+$ CD4$^+$ T cells in PBMC from naïve (open bars), VPEAR- (black bars) or RB51-vaccinated (gray bars) animals following (B) initial vaccination and (C) post-RB51 boost. (D) Frequency of IFN-γ$^+$ CD4$^+$ T cells in PBMC following stimulation with pokeweed mitogen as a positive control for IFN-γ production. Lower-case letters denote statistical significance between treatment groups at each individual timepoint, indicated by a p value ≤ 0.05.

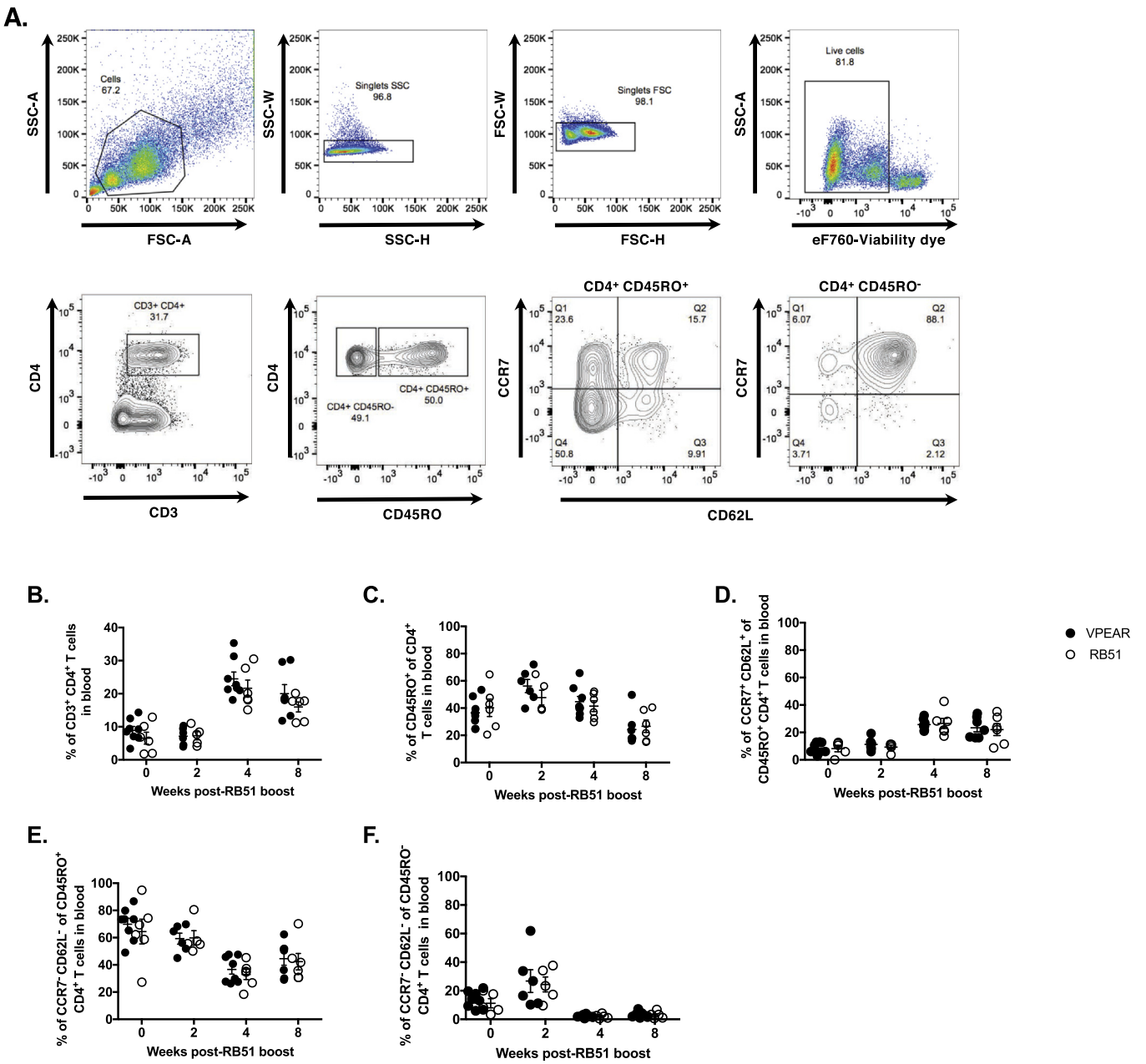

Fig. 2. Characterization of $CD4^+$ T cell subpopulations in PBMC following RB51 immunological challenge of VPEAR- and RB51-vaccinated animals. (A) Top panels are representative dot plots of PBMC analyzed *ex vivo* showing FSC vs. SSC profile and gating strategy for singlet discrimination and viability. Bottom panels are representative dot plots showing staining profiles with and gating strategies for CD3, CD4, CD45RO, CCR7 and CD62L. Shown are the kinetics of (B) total $CD4^+$ T cells, (C) $CD4^+$ memory T cells ($CD45RO^+$), (D) central memory $CD4^+$ T cells (T_{CM}: $CD45RO^+$ $CCR7^+$ $CD62L^+$), (E) effector memory $CD4^+$ T cells (T_{EM}: $CD45RO^+$ $CCR7^-$ $CD62L^-$), and (F) effector $CD4^+$ T cells (T_{eff}: $CD45RO^-$ $CCR7^-$ $CD62L^-$) in the peripheral blood of VPEAR- (black circles) and RB51-vaccinated (open circles) animals following RB51 immunological challenge or boost.

assessed memory subpopulations in PBMC before and after RB51 booster vaccination. We utilized CD45RO (a surface marker of memory T cells) and a combination of CCR7 (a chemokine receptor) and CD62L (a cell adhesion molecule) to distinguish between central memory (T_{CM}, $CCR7^+$ $CD62L^+$) and effector memory ($T_{EM:}$ $CCR7^+$ $CD62L^{low}$) $CD4^+$ T cells. Fig. 2A demonstrates the gating strategy and representative dot plots for the data. Overall, no differences ($p \geq 0.05$) were found between VPEAR and RB51 vaccinates at any of the time points or for any of the populations analyzed (Fig. 2).

However, we did observe changes in the circulating frequencies of memory subpopulations before and after RB51 boost. When compared to pre-RB51 boost frequencies, both vaccinate groups showed an increased frequency of total $CD4^+$ T cells at 4 and 8 weeks post-boost (Fig. 2B). Additionally, the mean percentage of $CD45RO^+$ $CD4^+$ memory T cells (Fig. 2C) appears to increase by 2 weeks post-boost, but was then decreased by 8 weeks post-boost. Within the circulating memory subset, we observed an increase in the mean frequency of T_{CM} cells (Fig. 2D) and a decrease in the mean frequency of T_{EM} (Fig. 2E) cells at 4 and 8 weeks post-boost. As expected for a memory response, we did not observe an increase in the mean frequency of $CD4^+$ T cells with an effector phenotype ($CD45RO^-$ $CCR7^-$ $CD62L^{-/low}$) (Fig. 2F). Overall, the kinetics of memory $CD4^+$ T cell subpopulations in both RB51 and VPEAR treatments groups were similar following RB51 boost.

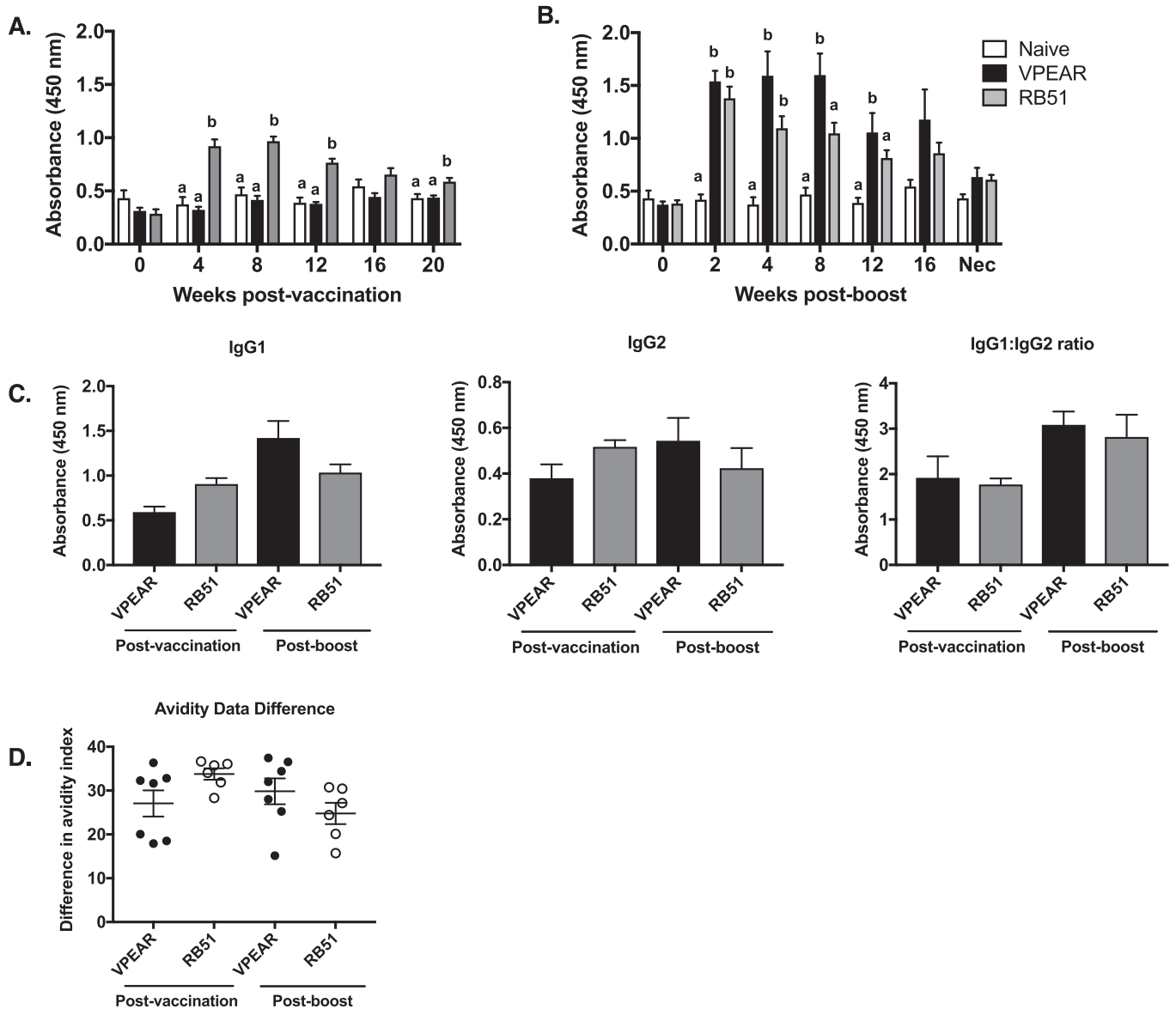

Fig. 3. Assessment of RB51-specific IgG titers in serum from VPEAR and RB51 vaccinated animals following initial vaccination and RB51 boost. Time course of RB51-specific total IgG in the serum of naïve (white bars), VPEAR- (black bars) and RB51-vaccinated (gray bars) animals at different time points following (A) initial vaccination and (B) RB51 boost. (C) Assessment of RB51-specific IgG isotypes, IgG1 and IgG2 in serum at 8 weeks post-initial vaccination and 8 weeks post-RB51 boost. (D) Assessment of RB51-specific IgG avidity at 8 weeks post-initial vaccination and 8 weeks post-RB51 boost Lower-case letters denote statistical significance between treatment groups at each individual timepoint, (*) denotes statistical significance as indicated by a p value ≤ 0.05.

3.4. RB51-specific IgG titers

Compared to naïve and VPEAR groups, mean IgG responses to RB51 after initial vaccination were increased ($p \leq 0.05$) at 4, 8, and 12 weeks post-vaccination (Fig. 3A). In contrast, humoral responses of animals in the VPEAR group did not differ ($p \geq 0.05$) from naïve animals at any of sampling times after initial vaccination.

As observed with $CD4^+$ T cell responses, we speculated that the initial vaccination with VPEAR was not sufficient to induce a measurable, peripheral IgG response. Therefore, we evaluated IgG responses after RB51 booster vaccination in both VPEAR and RB51 treatments. RB51-specific IgG increased ($p \leq 0.05$) at 4, 8, and 12 weeks post-RB51 boost in VPEAR and RB51 treatments compared to naïve animals (Fig. 3B). Additionally, at 8 weeks post-boost, there is a significant difference ($p \leq 0.05$) between mean IgG responses in the VPEAR- compared to RB51-vaccinated animals after booster vaccination. Titration curves were performed and area under the curve (AUC) values were calculated for various timepoints following RB51 boost to assess the quality of the antibody response (Supplemental Figure 2). Consistent with the above data, we observed statistically significant differences between vaccinates and naïve animals (2, 8 and 12 weeks post-boost), and between VPEAR- and RB51-vaccinates animals at 8 weeks post-boost (Supplemental Table 1).

We also assessed the IgG isotypes following initial vaccination and RB51 boost. At the time point analyzed, the predominant IgG isotype within sera of vaccinates was IgG1 (Fig. 3C), regardless of vaccination treatment.

3.5. Avidity of RB51-specific IgG responses

Previous work with this vaccination platform demonstrated an increase in antibody avidity over time (Schaut et al., 2018a). When evaluated at 8 weeks post-vaccination and 8 weeks post-boost, all vaccination

treatments demonstrated an expected loss of avidity with increasing concentrations of the chaotropic agent. However, antibody avidity did not differ ($p \geq 0.05$) between vaccination treatments (Fig. 3D).

3.6. Histology of implant sites

At necropsy, 15 months after initial vaccination, the site of implantation was grossly visible and palpable in all animals. Upon dissection, the VPEAR implant and rod were located within the subcutaneous space (Fig. 4A, top left), and grossly appeared surrounded by a fibrous capsule (Fig. 4A, top right and bottom left). Histologically, tissue immediately adjacent to the PVDF membrane cap of the implant demonstrated marked, moderately congested, radially oriented vascularization separated by streams of active, large fibroblasts in a collagen matrix (Fig. 4B). Variably sized islands of plasma cells were present within the central cap (Fig. 4B, C and D) accompanied frequently by hemosiderin pigment (Fig. 4D).

Surrounding the polymer rod were islands of moderate numbers of epithelioid macrophages with pronounced lymphocytic aggregates (Fig. 4E and F) interspersed within large streams of collagen fibers. Multinucleated giant cells were frequently observed stretching thinly around the polymer (Fig. 4G) and very large macrophages were found in the area of the rod appeared very large. Moderate numbers of eosinophils were also present (Fig. 4H). Rings of macrophages containing randomly dispersed eosinophils and small aggregates of lymphocytes encircled the rod (Fig. 4G). This was further surrounded by a halo of collagen bundles.

4. Discussion

The work presented in this manuscript characterizes the immune response elicited by a polyanhydride-based vaccination platform for extended antigen release in cattle and compares the immunologic responses to those elicited by vaccination with live RB51. The vaccine design is based on the phenomenon of concomitant immunity or non-sterile immunity (Coffman et al., 2010; Perignon and Druilhe, 1994; Smith et al., 1999). This phenomenon was mimicked by providing a three-hit model of antigen availability to the host: (1) soluble antigen, (2) a fast-eroding antigen-containing PA rod, and (3) a slow-eroding, antigen-containing PA rod and diffusion barrier. The dynamics of antigen presentation to the host via this platform would imitate a bolus of antigen availability after initial infection, followed by a slower release of antigen over a 3-month period and lastly, a slow release of antigen passively regulated by the formation of antigen-antibody complexes and hindered diffusion. We propose that altogether, this model would not only extend antigen release, it would mimic the dynamics of a persistent infection (i.e. controlled antigen release regulated by the immune response itself) without inducing tolerance to the antigen.

The VPEAR, PA rod and the polyethylene implant, was well tolerated as no clinical (i.e. swelling, drainage) or histologic evidence of adverse reactions were noted through the course of the study. An interesting finding was the observation of a large number of plasma cells adjacent to the implant cap, which was previously reported (Schaut et al., 2018a). To our knowledge, plasma cells are not typically recruited to the site of vaccination, suggesting this may be a unique feature of this vaccination platform and may be indicative of antibody production at the interphase between the host and the implant. This site was also characterized by a highly vascularized structure, suggesting active communication between the implant and the host at this interface. Notably, these findings are reminiscent of tertiary lymphoid structures, which can be induced by chronic immune stimulation. Tertiary lymphoid structures play an important role in the priming and maintenance of T and B cell responses in both inflammatory and infectious conditions (reviewed in (Neyt et al., 2012)). It would be of interest to further explore the dynamic interactions occurring at the site of implantation, and characterize the nature of the observed lymphoid aggregates at this site.

Immune responses after the initial placement of the VPEAR were very limited. In contrast, conventional vaccination with live RB51 induced peripheral, antigen-specific IFN-γ-producing $CD4^+$ T cell responses,

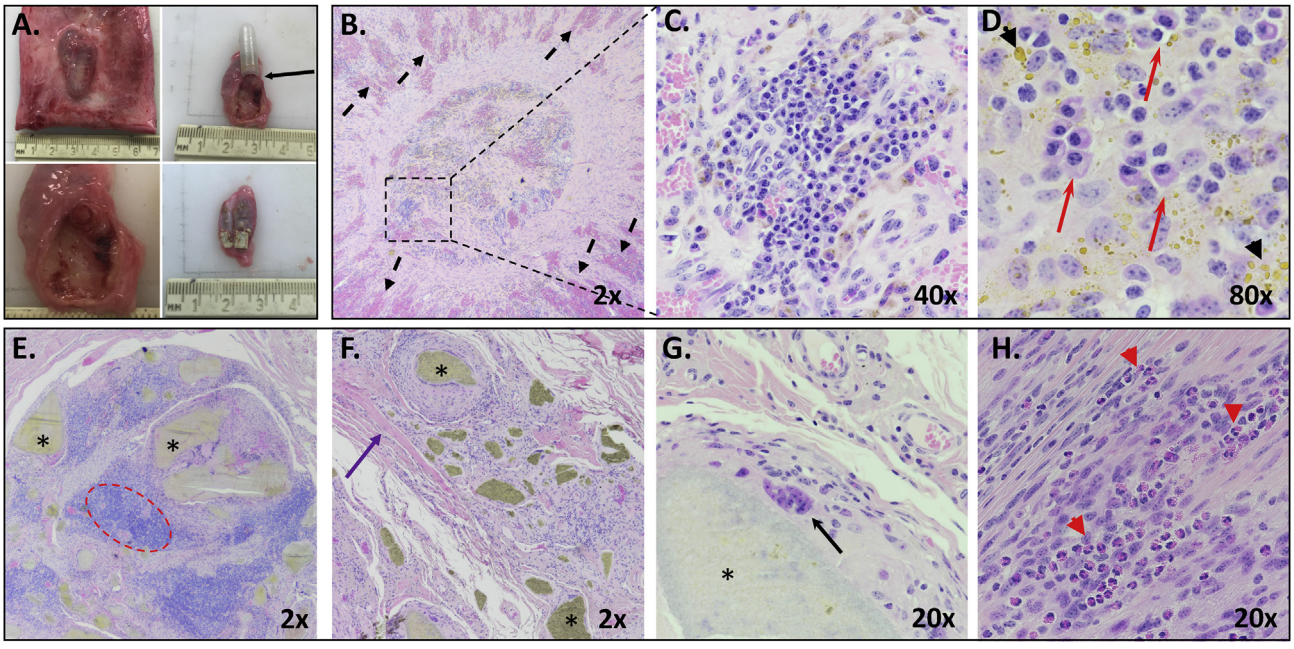

Fig. 4. Gross and histological images of implant and implant site. (A) Gross appearance of the implant and rod in the subcutaneous space (top left); appearance of implant on cut surface and connection of tissue at the PVDF membrane (top right, black arrow, and bottom left); and appearance of the rod on cut surface (bottom right). (B) Representative histology of the PVDF membrane cap site with radially-oriented vascularization separated by streams of fibroblasts and collagen (black dashed arrows) and multiple lymphocytic islands (dashed square). (C) Close up of lymphocytic island showing aggregates of plasma cells. (D) 80× image of plasma cells within cap site (red arrows) and hemosiderin pigment present throughout (black arrow heads). (E–H) Representative histology of the area surrounding the polymer rod (*), surrounded by islands of lymphocytes (dashed red circle), dense collagen (purple arrow), multinucleate giant cells (black arrow) and numerous eosinophils (red arrow heads).

measurable between 8-12 weeks and peaking at 16 weeks post-vaccination (Fig. 1A). The lack of $CD4^+$ T cell responses in the VPEAR treatment could be explained by: (1) the killed RB51 antigen was not a sufficient amount to elicit a cellular response; (2) the cellular response was not of the T_H1 type (i.e. T_H2, T_H17, T_{reg}/IL-10 mediated); (3) or the response was localized around the implant or within the draining lymph node. Therefore, we boosted all vaccinated animals with RB51 to test the hypothesis that VPEAR initiated and sustained an antigen-specific immune response *in vivo*.

Following RB51 boost, in both VPEAR- and RB51-vaccinated animals, the peak response was observed between 2-4 weeks post-boost, much earlier than with initial vaccination (8–16 weeks). This early response is consistent with an anamnestic rather than a primary response to antigen, suggesting that VPEAR- and RB51-vacinated animals had memory $CD4^+$ T cells capable of producing IFN-γ in response to RB51 boost. Similar to a previous report (Dorneles et al., 2015), following RB51 boost, we did not observe any measurable levels of IL-4 in culture supernatants in either vaccinate group (data not shown). Additionally, we measured IFN-γ, IL-10 and IL-17A at 2- and 4- weeks post-boost in culture supernatants, and observed no differences between the two vaccinate groups (Supplemental Figure 1). Altogether, these data demonstrate that the memory responses elicited by RB51 boost are similar between the two vaccinate groups.

Despite a lack of a measurable response after initial vaccination with VPEAR, there is a measurable anamnestic response, and similar to that observed in RB51-vaccinated animals. These data would support the hypothesis that VPEAR is capable of priming a RB51-specific, IFN-γ-mediated, $CD4^+$ T cell response in cattle. Previous work by Vitry et al. showed that in the mouse, the presence of IFN-γ-producing $CD4^+$ T_H1 cells requires immunization with live *Brucella* (Vitry et al., 2014). Historically, successful vaccines against brucellosis have been live attenuated strains as heat-killed or subcellular fractions fail to provide the same level of protection (Olsen, 2013). However, in our study, the magnitude and kinetics of the IFN-γ-mediated, $CD4^+$ T cell memory response of VPEAR-vaccinated animals is very similar to the memory response of RB51-vaccinated animals, following boost. Our data suggest that with this vaccine platform, it may be possible to elicit and sustain cellular responses against killed *Brucella* antigens without developing tolerance. However, it remains to be determined whether these cellular responses would be protective against challenge with field strains of *B. abortus*.

In an attempt to further characterize the kinetics of the secondary $CD4^+$ T cell response induced following RB51 boost, we analyzed the frequency of memory subpopulations in circulation. Overall, we did not observe any significant differences in any of the populations analyzed between VPEAR and RB51-vaccinated animals (Fig. 2). The magnitude and kinetics of memory $CD4^+$ T cell subpopulations following boost with RB51 appear very similar between the vaccinate groups, suggesting that both vaccines are capable of inducing T_{EM} and T_{CM}, which are known to be important for protection. Unfortunately, little is known regarding the memory T cell subsets that provide immunological protection against *Brucella* infection in cattle. Further understanding of memory subpopulations and their functional phenotypes that confer protection against *Brucella* are critical as we move forward with the development of this and other vaccine formulations against brucellosis.

Similar to the kinetics of the $CD4^+$ T cell response, an RB51-specific IgG response could not be detected following initial VPEAR vaccination. Animals vaccinated with RB51 showed an increase in RB51-specific IgG as early at 4 weeks post-vaccination, with decreasing titers by 16 weeks (Fig. 3), as previously reported (Olsen et al., 1999). As expected for an anamnestic response, following the RB51 boost, RB51-vaccinated animals respond by showing a significant increase in mean IgG titers. Interestingly, after RB51 boost, titers in VPEAR-vaccinated animals trended to be higher as compared to RB51-vaccinated animals, and were sustained out to 12 weeks post-boost. Again, these kinetics and magnitude are consistent with an anamnestic rather than a naïve response to RB51. We speculate that similar to the cellular responses, initial humoral responses to VPEAR may have remained localized to the site of implantation and/or lymph node. Histology data showing the recruitment of plasma cells to the implant cap support the localization of humoral responses to the vaccine site. Altogether, the data demonstrate that VPEAR is capable of initiating and sustaining humoral responses to killed RB51 antigen similar to live RB51.

Schaut et al. showed that in the mouse, this vaccine platform can maintain anti-GnRH antibody levels and enhances antibody avidity (Schaut et al., 2018a). While we did observe sustained anti-RB51 antibody titers following RB51 boost in the VPEAR- and RB51-vaccinated animals, we did not observe any differences in antibody avidity at the time point analyzed (8 weeks post vaccination and 8 weeks post-RB51 boost). This could be attributed to the nature of the antigen used between the two studies: purified protein vs. multiple antigenic peptide. Nevertheless, VPEAR and RB51 appear to have similar avidity indices at the timepoint analyzed.

The data presented here show that killed antigen could potentially be utilized to generate IFN-γ-mediated, $CD4^+$ T cell responses and humoral responses against *Brucella abortus* in its natural host. The rationale behind the design was to mimic the kinetics of antigen availability during persistent infections, which result in the development of concomitant immunity. To our knowledge, this novel approach to vaccination against persistent infections, such as *Brucella*, has not been attempted before. Further characterization of the observed cellular and humoral memory responses is warranted, along with studies to determine if vaccination with this platform can provide protection against challenge with field strains of *B. abortus*.

Declarations

Author contribution statement

Paola Boggiatto, Doug Jones: conceived and designed the experiments; performed the experiments; analyzed and interpreted the data; wrote the paper.

Robert Schaut, Carly Kanipe, Sean Kelly, Balaji Narasimhan: performed the experiments; wrote the paper.

Steven Olsen: Performed the experiments; analyzed and interpreted the data; wrote the paper.

Funding statement

This work was supported by the United States Department of Agriculture (USDA).

Competing interest statement

The authors declare no conflict of interest.

Additional information

Supplementary content related to this article has been published online at https://doi.org/10.1016/j.heliyon.2019.e02370.

Acknowledgements

Thank you to Dr. Catherine Vrentas, Lilia Walther, and Darl Pringle for their technical support. We would also like to thank Todd Pille, Craig Limkeman, and the Animal Resources Unit (ARU) at NADC for their assistance with animal husbandry, technical support, and sample collection. We thank Sam Humphrey at the NADC flow cytometry services, to Judi Stasko in histology services, and to Dr. Mitch Palmer for reviewing this manuscript.

References

Belkaid, Y., Piccirillo, C.A., Mendez, S., Shevach, E.M., Sacks, D.L., 2002. CD4+CD25+ regulatory T cells control Leishmania major persistence and immunity. Nature 420 (6915), 502–507.

Carrillo-Conde, B., Schiltz, E., Yu, J., Chris Minion, F., Phillips, G.J., Wannemuehler, M.J., Narasimhan, B., 2010. Encapsulation into amphiphilic polyanhydride microparticles stabilizes Yersinia pestis antigens. Acta Biomater. 6 (8), 3110–3119.

Cheville, N.F., Olsen, S.C., Jensen, A.E., Stevens, M.G., Palmer, M.V., Florance, A.M., 1996. Effects of age at vaccination on efficacy of Brucella abortus strain RB51 to protect cattle against brucellosis. Am. J. Vet. Res. 57 (8), 1153–1156. https://www.ncbi.nlm.nih.gov/pubmed/8836366.

Cheville, N.F., Stevens, M.G., Jensen, A.E., Tatum, F.M., Halling, S.M., 1993. Immune responses and protection against infection and abortion in cattle experimentally vaccinated with mutant strains of Brucella abortus. Am. J. Vet. Res. 54 (10), 1591–1597. https://www.ncbi.nlm.nih.gov/pubmed/8250382.

Coffman, R.L., Sher, A., Seder, R.A., 2010. Vaccine adjuvants: putting innate immunity to work. Immunity 33 (4), 492–503.

Cossaboom, C.M., Kharod, G.A., Salzer, J.S., Tiller, R.V., Campbell, L.P., Wu, K., Stonecipher, S., 2018. Notes from the field: Brucella abortus vaccine strain RB51 infection and exposures associated with raw milk consumption - wise County, Texas, 2017. MMWR Morb. Mortal. Wkly. Rep. 67 (9), 286.

Dorneles, E.M., Lima, G.K., Teixeira-Carvalho, A., Araujo, M.S., Martins-Filho, O.A., Sriranganathan, N., Lage, A.P., 2015. Immune response of calves vaccinated with Brucella abortus S19 or RB51 and revaccinated with RB51. PLoS One 10 (9) e0136696.

Haughney, S.L., Petersen, L.K., Schoofs, A.D., Ramer-Tait, A.E., King, J.D., Briles, D.E., Narasimhan, B., 2013. Retention of structure, antigenicity, and biological function of pneumococcal surface protein A (PspA) released from polyanhydride nanoparticles. Acta Biomater. 9 (9), 8262–8271.

Huang, L., Krieg, A.M., Eller, N., Scott, D.E., 1999. Induction and regulation of Th1-inducing cytokines by bacterial DNA, lipopolysaccharide, and heat-inactivated bacteria. Infect. Immun. 67 (12), 6257–6263. https://www.ncbi.nlm.nih.gov/pubmed/10569735.

Huang, L.Y., Aliberti, J., Leifer, C.A., Segal, D.M., Sher, A., Golenbock, D.T., Golding, B., 2003. Heat-killed Brucella abortus induces TNF and IL-12p40 by distinct MyD88-dependent pathways: TNF, unlike IL-12p40 secretion, is Toll-like receptor 2 dependent. J. Immunol. 171 (3), 1441–1446. https://www.ncbi.nlm.nih.gov/pubmed/12874236.

Huang, L.Y., Ishii, K.J., Akira, S., Aliberti, J., Golding, B., 2005. Th1-like cytokine induction by heat-killed Brucella abortus is dependent on triggering of TLR9. J. Immunol. 175 (6), 3964–3970. https://www.ncbi.nlm.nih.gov/pubmed/16148144.

Huntimer, L., Ramer-Tait, A.E., Petersen, L.K., Ross, K.A., Walz, K.A., Wang, C., Wannemuehler, M.J., 2013. Evaluation of biocompatibility and administration site reactogenicity of polyanhydride-particle-based platform for vaccine delivery. Adv. Healthc. Mater. 2 (2), 369–378.

Mandell, M.A., Beverley, S.M., 2017. Continual renewal and replication of persistent Leishmania major parasites in concomitantly immune hosts. Proc. Natl. Acad. Sci. U. S. A. 114 (5), E801–E810.

Marianelli, C., Ciuchini, F., Tarantino, M., Pasquali, P., Adone, R., 2004. Genetic bases of the rifampin resistance phenotype in Brucella spp. J. Clin. Microbiol. 42 (12), 5439–5443.

Montaraz, J.A., Winter, A.J., 1986. Comparison of living and nonliving vaccines for Brucella abortus in BALB/c mice. Infect. Immun. 53 (2), 245–251. https://www.ncbi.nlm.nih.gov/pubmed/3089933.

Neyt, K., Perros, F., GeurtsvanKessel, C.H., Hammad, H., Lambrecht, B.N., 2012. Tertiary lymphoid organs in infection and autoimmunity. Trends Immunol. 33 (6), 297–305.

Nicolas, L., Sidjanski, S., Colle, J.H., Milon, G., 2000. Leishmania major reaches distant cutaneous sites where it persists transiently while persisting durably in the primary dermal site and its draining lymph node: a study with laboratory mice. Infect. Immun. 68 (12), 6561–6566. https://www.ncbi.nlm.nih.gov/pubmed/11083765.

Olsen, S.C., 2000. Immune responses and efficacy after administration of a commercial Brucella abortus strain RB51 vaccine to cattle. Vet. Ther. 1 (3), 183–191. https://www.ncbi.nlm.nih.gov/pubmed/19757581.

Olsen, S.C., 2013. Recent developments in livestock and wildlife brucellosis vaccination. Rev. Sci. Tech. 32 (1), 207–217. https://www.ncbi.nlm.nih.gov/pubmed/23837378.

Olsen, S.C., Boyle, S.M., Schurig, G.G., Sriranganathan, N.N., 2009. Immune responses and protection against experimental challenge after vaccination of bison with Brucella abortus strain RB51 or RB51 overexpressing superoxide dismutase and glycosyltransferase genes. Clin. Vaccine Immunol. 16 (4), 535–540.

Olsen, S.C., Bricker, B., Palmer, M.V., Jensen, A.E., Cheville, N.F., 1999. Responses of cattle to two dosages of Brucella abortus strain RB51: serology, clearance and efficacy. Res. Vet. Sci. 66 (2), 101–105.

Olsen, S.C., Stoffregen, W.S., 2005. Essential role of vaccines in brucellosis control and eradication programs for livestock. Expert Rev. Vaccines 4 (6), 915–928.

Palmer, M.V., Olsen, S.C., Cheville, N.F., 1997. Safety and immunogenicity of Brucella abortus strain RB51 vaccine in pregnant cattle. Am. J. Vet. Res. 58 (5), 472–477. https://www.ncbi.nlm.nih.gov/pubmed/9140553.

Perignon, J.L., Druilhe, P., 1994. Immune mechanisms underlying the premunition against Plasmodium falciparum malaria. Mem. Inst. Oswaldo Cruz 89 (Suppl 2), 51–53. https://www.ncbi.nlm.nih.gov/pubmed/7565132.

Petersen, L.K., Xue, L., Wannemuehler, M.J., Rajan, K., Narasimhan, B., 2009. The simultaneous effect of polymer chemistry and device geometry on the in vitro activation of murine dendritic cells. Biomaterials 30 (28), 5131–5142.

Poester, F.P., Goncalves, V.S., Paixao, T.A., Santos, R.L., Olsen, S.C., Schurig, G.G., Lage, A.P., 2006. Efficacy of strain RB51 vaccine in heifers against experimental brucellosis. Vaccine 24 (25), 5327–5334.

Ross, K.A., Loyd, H., Wu, W., Huntimer, L., Ahmed, S., Sambol, A., Narasimhan, B., 2015. Hemagglutinin-based polyanhydride nanovaccines against H5N1 influenza elicit protective virus neutralizing titers and cell-mediated immunity. Int. J. Nanomed. 10, 229–243.

Ross, K.A., Loyd, H., Wu, W., Huntimer, L., Wannemuehler, M.J., Carpenter, S., Narasimhan, B., 2014. Structural and antigenic stability of H5N1 hemagglutinin trimer upon release from polyanhydride nanoparticles. J. Biomed. Mater. Res. A 102 (11), 4161–4168.

Schaut, R.G., Brewer, M.T., Hostetter, J.M., Mendoza, K., Vela-Ramirez, J.E., Kelly, S.M., Jones, D.E., 2018a. A single dose polyanhydride-based vaccine platform promotes and maintains anti-GnRH antibody titers. Vaccine 36 (7), 1016–1023.

Schaut, R.G., Brewer, M.T., Mendoza, K., Jackman, J., Narasimhan, B., Jones, D.E., 2018b. A polyanhydride-based implantable single dose vaccine platform for long-term immunity. Vaccine 36 (7), 1024–1025.

Schurig, G.G., Roop 2nd, R.M., Bagchi, T., Boyle, S., Buhrman, D., Sriranganathan, N., 1991. Biological properties of RB51; a stable rough strain of Brucella abortus. Vet. Microbiol. 28 (2), 171–188. https://www.ncbi.nlm.nih.gov/pubmed/1908158.

Smith, T., Felger, I., Tanner, M., Beck, H.P., 1999. Premunition in Plasmodium falciparum infection: insights from the epidemiology of multiple infections. Trans. R. Soc. Trop. Med. Hyg. 93 (Suppl 1), 59–64. https://www.ncbi.nlm.nih.gov/pubmed/10450428.

Torres, M.P., Vogel, B.M., Narasimhan, B., Mallapragada, S.K., 2006. Synthesis and characterization of novel polyanhydrides with tailored erosion mechanisms. J. Biomed. Mater. Res. A 76 (1), 102–110.

Ulery, B.D., Kumar, D., Ramer-Tait, A.E., Metzger, D.W., Wannemuehler, M.J., Narasimhan, B., 2011a. Design of a protective single-dose intranasal nanoparticle-based vaccine platform for respiratory infectious diseases. PLoS One 6 (3) e17642.

Ulery, B.D., Petersen, L.K., Phanse, Y., Kong, C.S., Broderick, S.R., Kumar, D., Narasimhan, B., 2011b. Rational design of pathogen-mimicking amphiphilic materials as nanoadjuvants. Sci. Rep. 1, 198.

Vela Ramirez, J.E., Roychoudhury, R., Habte, H.H., Cho, M.W., Pohl, N.L., Narasimhan, B., 2014. Carbohydrate-functionalized nanovaccines preserve HIV-1 antigen stability and activate antigen presenting cells. J. Biomater. Sci. Polym. Ed. 25 (13), 1387–1406.

Vela-Ramirez, J.E., Goodman, J.T., Boggiatto, P.M., Roychoudhury, R., Pohl, N.L., Hostetter, J.M., Narasimhan, B., 2015. Safety and biocompatibility of carbohydrate-functionalized polyanhydride nanoparticles. AAPS J. 17 (1), 256–267.

Vitry, M.A., Hanot Mambres, D., De Trez, C., Akira, S., Ryffel, B., Letesson, J.J., Muraille, E., 2014. Humoral immunity and CD4+ Th1 cells are both necessary for a fully protective immune response upon secondary infection with Brucella melitensis. J. Immunol. 192 (8), 3740–3752.

Yazdi, H.S., Kafi, M., Haghkhah, M., Tamadon, A., Behroozikhah, A.M., Ghane, M., 2009. Abortions in pregnant dairy cows after vaccination with Brucella abortus strain RB51. Vet. Rec. 165 (19), 570–571.

Zhan, Y., Kelso, A., Cheers, C., 1993. Cytokine production in the murine response to brucella infection or immunization with antigenic extracts. Immunology 80 (3), 458–464. https://www.ncbi.nlm.nih.gov/pubmed/8288319.

Zhan, Y., Kelso, A., Cheers, C., 1995. Differential activation of Brucella-reactive CD4+ T cells by Brucella infection or immunization with antigenic extracts. Infect. Immun. 63 (3), 969–975. https://www.ncbi.nlm.nih.gov/pubmed/7868269.